Optimal Selection of Power Converter in DFIG Wind Turbine With Enhanced System-Level Reliability

Zhou, Dao; Zhang, Guanguan; Blaabjerg, Frede

Published in:
I E E E Transactions on Industry Applications

DOI (link to publication from Publisher):
10.1109/TIA.2018.2822239

Publication date:
2018

Document Version
Accepted author manuscript, peer reviewed version

Citation for published version (APA):
Zhou, D., Zhang, G., & Blaabjerg, F. (2018). Optimal Selection of Power Converter in DFIG Wind Turbine With Enhanced System-Level Reliability. *I E E E Transactions on Industry Applications*, *54*(4), 3637 - 3644. https://doi.org/10.1109/TIA.2018.2822239

This article has been accepted for publication in a future issue of this journal, but has not been fully edited. Content may change prior to final publication. Citation information: DOI 10.1109/TIA.2018.2822239, IEEE Transactions on Industry Applications

Optimal Selection of Power Converter in DFIG Wind Turbine with Enhanced System-level Reliability

Dao Zhou
Member, IEEE
Department of Energy Technology
Aalborg University
Pontoppidanstraede 101
Aalborg, DK-9220, Denmark
zda@et.aau.dk

Guanguan Zhang
Student Member, IEEE
School of Information Science and Technology
Central South University
Lushan South Road 932
Changsha, 410083, China
dr_zgg@163.com

Frede Blaabjerg
Fellow, IEEE
Department of Energy Technology
Aalborg University
Pontoppidanstraede 101
Aalborg, DK-9220, Denmark
fbl@et.aau.dk

***Abstract* - With the increasing penetration of wind power, reliable and cost-effective wind energy production is of more and more importance. As one of the common configurations, the doubly-fed induction generator based partial-scale wind power converter is still dominating in the existing wind farms, and its reliability assessment is studied considering the annual wind profile. According to an electro-thermal stress evaluation, the time-to-failure of the key power semiconductors is predicted by using lifetime models and Monte Carlo based variation analysis. Aiming for the system-level reliability analysis, a reliability block diagram can be used based on Weibull distributed component-level reliability. A case study of a 2 MW wind power converter shows that the optimal selection of power module may be different seen from the reliability perspective compared to the electrical stress margin. It can also be seen that the B_1 lifetimes of the grid-side converter and the rotor-side converter deviate a lot by considering the electrical stresses, while they become more balanced by using an optimized design strategies. Thus, the system-level lifetime increases significantly with an appropriate design of the back-to-back power converters.**

***Index Terms* - System-level reliability, wind power, doubly-fed induction generator, power electronics, Monte Carlo analysis, reliability block diagram.**

I. INTRODUCTION

With the increasing penetration of wind power during recent decades, the reliable and cost-effective wind energy production is of more and more importance [1]-[3]. As the modern wind turbine is required to act like the conventional synchronous generator with independent reactive and active power regulation, the power electronics are nowadays playing an important role even to the full-scale of the turbine generator. In order to reduce the cost of the wind power generation, the power rating of the individual wind turbine is up-scaled to 8 MW and even above. However, the feedback from the wind turbine market indicates that the best-seller is still those rated around 2-3 MW, in which the Doubly-Fed Induction Generator (DFIG) is normally employed together with partial-scale power electronic converters [4]. Another tendency of the wind power development is the popularity of the offshore wind farms, which pushes the wind turbine system to operate with reliable performance due to the high maintenance cost.

Reliability and robustness of the system are closely related to its mission profile - the representation of all relevant conditions that the system will be exposed to in all of its intended application throughout its entire life cycle [5], [6]. The failure usually happens during the overlap between the stress and strength distribution [7], [8]. The stress is related to the environmental loads (like thermal, mechanical, humidity, etc.), or the functional loads (such as user profiles, electrical operation) [9]-[12]. On the other hand, the strength means the ability to endure such stressors before fatigue occurs (e.g. the boundary between the elastic and plastic deformations in connection with the thermal-mechanical stress). In respect to the power electronic converter, the IGBT power module is commonly regarded as one of the fragile components. The power modules are subjected to a variety of temperature profiles, which cause cyclic thermo-mechanical stress in all the components and joints of the modules and finally lead to device failure. Due to the considerably thermal expansion coefficients difference among the module layers, the bond wires, chip solder joints and substrate solder joints suffer most from the thermal stress. As discussed in [13], the lifetime model for the solder joint is based on the time-dependent creep and therefore the cycle period affects the solder joint lifetime. However, the lifetime model for the bond wire is independent with the cycle period, as this model assumes that the immediate plastic deformation leads to fatigue instead of the time-dependent creep. Besides, there are two kinds of thermal cycles in the wind power generation [14], [15]. One is the loading variation based thermal cycles, which are caused by changing wind speed and ambient temperature with cycle period from seconds to years. The other is fundamental-frequency based thermal cycles ranging from milliseconds to seconds, which are induced by the complementary conduction between the IGBTs and the freewheeling diodes within a

This article has been accepted for publication in a future issue of this journal, but has not been fully edited. Content may change prior to final publication. Citation information: DOI 10.1109/TIA.2018.2822239, IEEE Transactions on Industry Applications

fundamental frequency of the ac current through the power converter. Their effects on lifetime consumption have been studied in [14], and the fundamental-frequency based thermal cycle effects on the chip fatigue are the main focus of this paper.

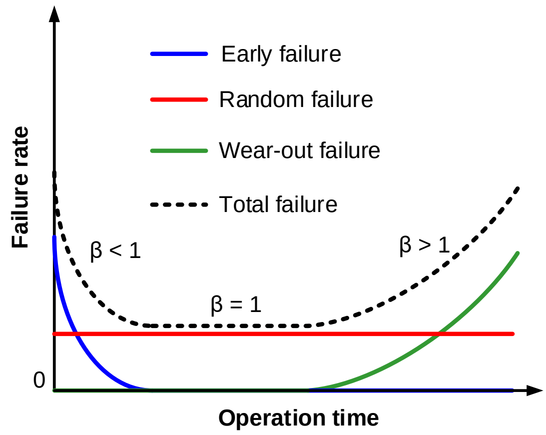

(a)

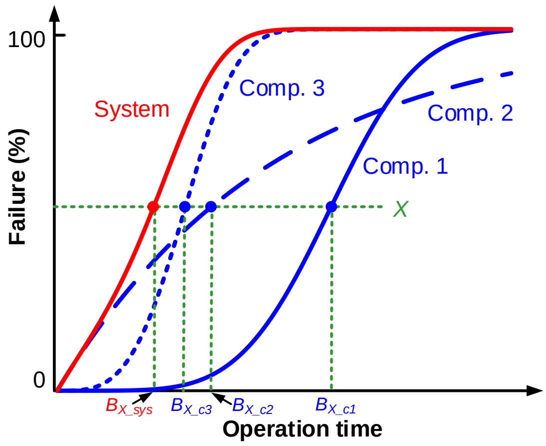

(b)

Fig. 1. Common concepts used in reliability engineering statistics. (a) Failure rate along with operation time. (b) Failure curve with operation time from component to system.

A typical failure rate curve against the time in the lifecycle of a power electronics product is plotted in Fig. 1(a), which is composed of three reliability functions and it is known as the "Bathtub curve" [7]. By examining the fitting parameters β in the Weibull reliability functions, three types of failures that are dominant at different stages of the lifecycle can be identified. The first part is dominant by early failures caused by "infant mortality" with a decreasing failure rate ($\beta < 1$). The second part is dominant by random failures in the useful life of a product with a constant failure rate ($\beta = 1$). The third part is dominant by wear-out failures at the end of life of the product with an increasing failure rate ($\beta > 1$). The failure rate determined by using exponential distribution is applied from various handbooks [16], [17]. This method is simple and inappropriate, considering only the operation period with a constant failure rate but neglecting the wear-out phase. Due to limited failure data provided by manufacturers, only the percentile lifetime can be obtained, which indicates the B_X lifetime (X% among the total samples or X% probability of a product will fail at this operational time). As illustrated in Fig. 1(b), the B_X lifetime is merely a particular point without the complete information of the unreliability or failure curve. Under this circumstance, although the B_X lifetime of all components in the system is well known, the effect on the system-level reliability from each component cannot be reflected, where the system lifetime is roughly determined by the lifetime of the most fragile component. Consequently, an approach to bridge the gap from the percentile lifetime to the complete reliability curve is highly demanded. In practice, there are parameter variations in the applied components and corresponding lifetime models, and a certain degree of uncertainties in the environmental and operating conditions. Therefore, the time-to-failure of the individual components is distributed within a certain range. The numerical results can be obtained by using Monte Carlo analysis, a broad class of computational algorithms that rely on repeated random samplings [7]. Afterwards, the parameters of the Weibull distribution, which it is a widely used statistical distribution to represent large samples of life data [18], can be estimated by means of curve fitting.

Based on component-level reliability metrics, the system-level reliability can be derived by using the Reliability Block Diagram (RBD), the Fault Tree Analysis (FTA), and the Markov Chain (MC) [19]-[25]. In [19]-[21], the reliability of an interleaved dc/dc boost converter, an induction motor drive, and a PEM fuel cell power plant are evaluated using the MC method. In addition, the RBD approach is used to analyze the reliability of a paralleled inverter system [22]. However, a constant failure rate is applied, which neglects the effects introduced by the wear-out stage. An FTA for the PEM fuel cell is performed in [23], where again a constant failure rate is assumed. However, this research very seldom considers the mission profile.

The background of this paper is related to the power converter design in a 2 MW DFIG wind turbine, which requires a balanced lifetime between the back-to-back power converters with enhanced system-level reliability. The motivation is to predict the reliability of the power converter at the end of service life to better size the key power modules for the next generation product design. The outcome of the study is used to assist the design phase of product development. The novel aspects of the proposed method of the reliability evaluation are as follows: 1) obtain the time-to-failure distribution of the power module considering parameter variations in both applied components and corresponding lifetime models, and 2) define the new design criteria of power modules seen from the reliability perspective other than the electrical stresses margin.

The structure of the paper is outlined as follows. Section II analyzes the electrical stresses of the DFIG Back-To-Back (BTB) power converters and discusses the possibilities of the power modules selection. Section III and IV evaluate the

This article has been accepted for publication in a future issue of this journal, but has not been fully edited. Content may change prior to final publication. Citation information: DOI 10.1109/TIA.2018.2822239, IEEE Transactions on Industry Applications

reliability of the individual power semiconductor and the BTB power converters with various power module selections. Finally, concluding remarks are drawn in the last section.

II. Electrical Stresses and Selected Power Devices

As shown in Fig. 2, one of the mainstream configurations in the wind turbine market is equipped with the DFIG. Since the rotor-side of the generator only handles the slip power of the stator-side, the partial-scale BTB power converters are employed, which are named as the Rotor-Side Converter (RSC) and the Grid-Side Converter (GSC) due to their positions. Although the same amount of active power flows through the RSC and GSC, the DFIG is normally excited from the rotor-side in order to guarantee a unity power factor to the power grid. Additionally, the various interfacing voltage and operating frequency of the RSC and GSC force different electrical stresses of the used power devices (the IGBT and the diode of the RSC and the GSC: RT, RD, GT, and GD, respectively). As a result, this section is served to analyze the stresses of the power devices and help to select their suitable paralleled numbers for the rated power.

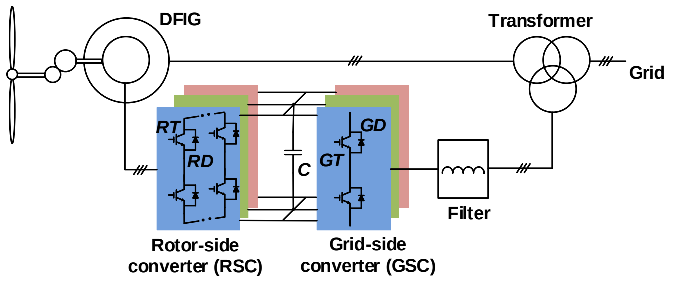

Fig. 2. Back-to-back power converters in the doubly-fed induction generator (DFIG) based wind turbine system.

The interfacing voltage and flowing current of the RSC are heavily dependent on the inherent parameters of the DFIG. Neglecting the stator resistance and the rotor resistance, and together with the help of DFIG modeling in the *dq* reference frame [9], the relationship between the rotor-side voltage u_r and current i_r and the stator-side voltage u_s and current i_s are,

$$i_r^{'} = -\frac{L_s}{L_m} i_{sd} - j(\frac{U_s}{\omega_1 L_m} + \frac{L_s}{L_m} i_{sq}) \tag{1}$$

$$u_r^{'} = s(\frac{L_r}{L_m} U_s + \frac{\sigma \omega_1 L_r L_s}{L_m} i_{sq}) - js\frac{\sigma \omega_1 L_r L_s}{L_m} i_{sd} \tag{2}$$

where U_s denotes the stator voltage, ω_1 denotes the stator angular frequency, L_s, L_m and L_r denote the stator inductance, magnetizing inductance and rotor inductance, respectively, σ denotes the leakage coefficient, defined as $(L_sL_r-L_m^2)/L_m^2$, s is the slip of the induction generator. It is worth noting that the superscript *'* means the rotor values are referred to the stator side, while subscripts *d* and *q* represent the values in the d-axis and q-axis.

In respect to the GSC, if a single inductor L_g is used as the grid filter, the voltage v_g and current i_g of the GSC can be expressed as,

$$i_g = i_{gd} + ji_{gq} \tag{3}$$

$$u_g = U_{gr} + \omega_1 L_g i_{gq} - j\omega_1 L_g i_{gd} \tag{4}$$

where U_{gr} denotes the grid voltage.

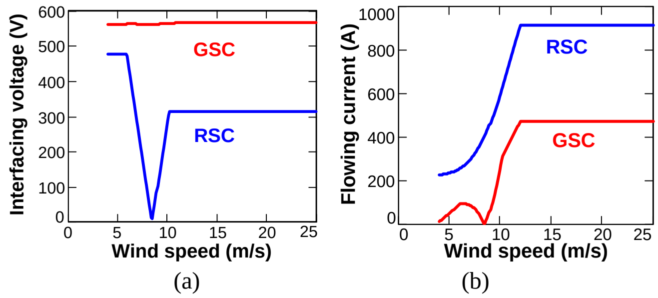

Fig. 3. Electrical stresses of RSC and GSC along with the wind speed. (a) Converter interfacing voltage. (b) Converter current loading.

Table I

Parameters of 2 MW DFIG System

DFIG	
Rated power P_n [kW]	2000
Rated electrical frequency f_1 [Hz]	50
Slip range s	-0.2 ~ 0.3
Phase peak voltage U_{gr} /U_s [V]	563
Stator leakage inductance L_s [mH]	2.95
Rotor leakage inductance L_r [mH]	2.97
Magnetizing inductance L_m [mH]	2.91
Turns ratio k_{sr}	0.369
Power converter	
DC-link voltage U_{dc} [V]	1050
Switching frequency f_s [kHz]	2
Filter inductance L_g [mH]	0.5

A case study is performed at a 2 MW DFIG system, and the parameters are listed in Table I. It is noted that the switching frequency of the GSC and RSC are both set at 2 kHz, and the dc-link voltage is kept at 1050 V.

In the case that the power curve of the wind turbine follows the maximum power point tracking, the interfacing voltage and flowing current of the BTB power converters can be calculated according to (1)-(4). As shown in Fig. 3, it is evident that the RSC voltage is much lower than the GSC, as the GSC provides the voltage similar to the power grid, while the generated RSC voltage is roughly the product of the slip and stator voltage over the winding ratio between the stator and the rotor. As a result, the rotor voltage is lowest around the synchronous operation of the DFIG. Due to a much lower voltage of the RSC, it can be expected that the rotor current becomes higher because the same active power flows through the BTB power converters. Moreover, the RSC supports the

This article has been accepted for publication in a future issue of this journal, but has not been fully edited. Content may change prior to final publication. Citation information: DOI 10.1109/TIA.2018.2822239, IEEE Transactions on Industry Applications

excitation power from the rotor side, which even imposes on the stress of the rotor current.

In order to the implement common low-voltage power semiconductors existing in the market, the 1 kA/1.7 kV power modules can be used for the BTB power converters. The single half-bridge module can be selected for each arm of the GSC, while two half-bridge modules need to be connected in parallel to ensure a similar current margin between the RSC and the GSC.

III. Lifetime Distribution of Individual Power Device

Based on the interfacing voltage and flowing current of the BTB power converters, the thermal stress of the power devices can be evaluated. This section will investigate the component-level reliability, where the lifetime estimation and distribution of each power device are in focus.

A. Lifetime estimation of power devices

The general procedure from the wind turbine specification to the lifetime estimation of power devices is shown in Fig. 4, which consists of five major steps [12], [13]. According to the wind turbine specification (e.g. the effective wind speed range, maximum and minimum turbine speed, turbine radius and rated power), the turbine output power and rotor speed in the relationship with the wind speed can be obtained with the gearbox ratio. On the basis of the DFIG and grid-tied converter models, the voltage, current, and the displacement angle of the power converters can be calculated. Then, the loss dissipation of the power semiconductors can be deduced with the operation conditions of the power device (e.g. the switching frequency, commutation voltage). Afterwards, the junction temperature swing and the mean junction temperature can be anticipated based on the thermal resistance and capacitance of the power device as well as its cooling method. Eventually, the annual damage of the device can be calculated by using the annual thermal cycles, where the annual wind profile is taken into account, over the cycle-to-failure derived from the Bayerer's lifetime model of the power device [26]. Assuming a repetitive annual mission profile, the reciprocal of the annual damage indicates the lifespan of the studied power device.

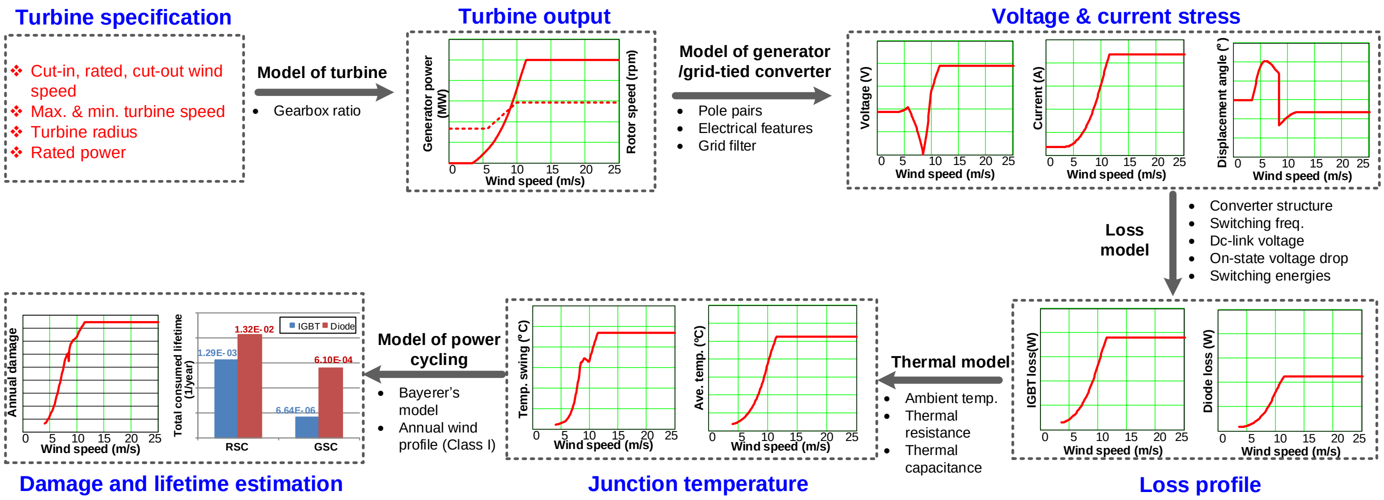

Fig. 4. General procedure from turbine specification to lifetime estimation of power devices.

Due to the limited lifetime data of the power semiconductors, the above calculation is the B_{10} lifetime, which means 10% of the power semiconductors fail at the estimated lifetime. Under this circumstance, the lifetime of the power converter can only be determined by the most stressed power device, and the effects of other power semiconductors on the system-level reliability cannot be evaluated. Besides, in the reliability-critical applications, the B_5 or even the B_1 lifetime may be required. However, they cannot be predicted in this condition.

B. Lifetime distribution of power devices

In order to perform the reliability assessment towards the power converter level, an approach to analyze the lifetime distribution of the power device will be addressed and described. The previous discussion gives a B_{10} annual damage of power devices, but the uncertainties due to the statistical properties of the applied lifetime model and the parameter variations of the power device are not taken into account. Therefore, a statistical approach to analyze the lifetime performance subject to parameter variations is carried out in details by means of Monte Carlo analysis. Finally, the time-to-failure distribution of the power semiconductors can be estimated.

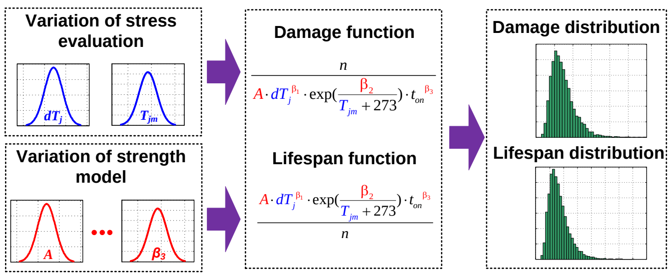

Fig. 5. Flowchart of the Monte Carlo analysis for lifespan estimation.

This article has been accepted for publication in a future issue of this journal, but has not been fully edited. Content may change prior to final publication. Citation information: DOI 10.1109/TIA.2018.2822239, IEEE Transactions on Industry Applications

Since the lifetime data are obtained from the accelerated results based on a specific number of testing samples, there is a certain degree of uncertainty of the derived constant parameters. As mentioned in [26], the coefficients of the Bayerer's model are fitted by a large number of test data:

$$N_f = A \cdot dT_j^{\beta_1} \cdot \exp\left(\frac{\beta_2}{T_{jm}+273}\right) \cdot t_{on}^{\beta_3} \tag{5}$$

where the power cycles are closely related to the junction temperature swing dT_j, the mean junction temperature T_{jm} as well as its on-time duration t_{on}. Besides, A, β_1, β_2 and β_3 can be obtained according to test data provided by the manufacturer of the device. All the parameters in the lifetime model as stated in (5) are distributed by means of a Normal probability density function (pdf), assuming that A, β_1, β_2 and β_3 experience a variation of 5%. It is worth noting that such variations may differ from power semiconductor manufacturers. The second type of uncertainty exists due to variances in the manufacturing process (like the typical, maximum and minimum on-state resistance of the IGBT and the freewheeling diode), which results in the variation of the mean junction temperature and the junction temperature fluctuation. In order to illustrate this, the diode of the RSC is selected as an example. To simplify the varying junction temperature profile around the year, the equivalent static values of the junction temperature swing of the power device can be calculated by the annual average wind speed and its corresponding mean junction temperature as listed in Table II.

Table II

EQUIVALENT STATIC VALUE FOR EACH POWER SEMICONDUCTOR

Devices in converter	RD	RT	GD	GT
Number of cycles per year n	3.15E8	3.15E8	1.58E9	1.58E9
Annual damage D	1.32E-2	1.29E-3	6.10E-4	6.64E-6
Number of cycles to failure N_f	2.39E10	2.44E11	2.58E12	2.37E14
Mean junction temperature T_{jm} [ºC]	68.3	68.6	69.0	64.6
On-state time t_{on} [S]	0.05	0.05	0.01	0.01
Junction temperature swing dT_j [ºC]	11.7	7.3	5.3	2.3

Similar as the uncertainties in the Bayerer's lifetime model, assuming a variation of 5% of the junction temperature fluctuation and the mean junction temperature, the annual damage distribution can be calculated by using Monte Carlo analysis, as shown in Fig. 5. As the accuracy of the output distribution depends on sample numbers [7], 10,000 samplings are chosen in this case study.

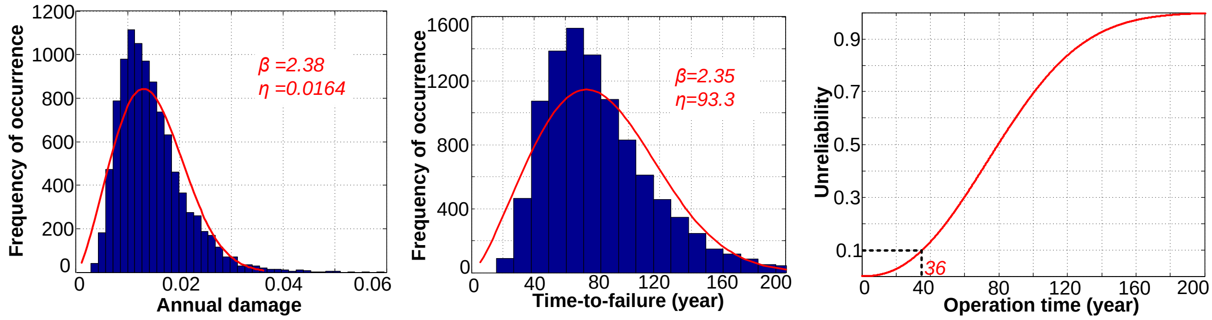

(a) (b) (c)

Fig. 6. Monte Carlo analysis considering all parameter variations of the diode in the rotor-side converter. (a) Probability density function (pdf) of annual damage; (b) End-of-life probability density function; (c) Accumulated percentage of failure along with the operation time.

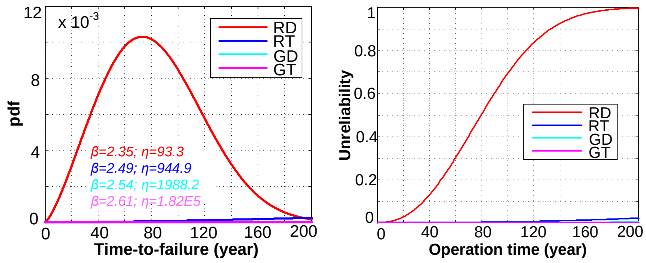

(a) (b)

Fig. 7. Unreliability of diodes and IGBTs in the back-to-back power converters. (a) End-of-life probability density function. (b) Accumulated percentage of failure along with the operation time.

Note: RD, RT, GD and GT stand for diode of RSC, transistor of RSC, diode of GSC, and transistor of GSC, respectively.

It is well-known that the time-to-failure data typically follows the Weibull distribution [18], whose pdf follows,

$$f(t) = \frac{\beta}{\eta}\left(\frac{t}{\eta}\right)^{\beta-1} \cdot \exp\left[-\left(\frac{t}{\eta}\right)^{\beta}\right] \tag{6}$$

where η and β denote the scale and shape parameters of the Weibull distribution.

As depicted in Fig. 6(a), the fitting curve of annual damage can be obtained with a scale parameter of 0.0164 and a shape parameter of 2.38. Assuming the repetitive annual mission profile, the probability of the lifetime is distributed as shown in Fig. 6(b). Then, the unreliability of the power device can be deduced in Fig. 6(c), which is the integration of the failure pdf. It is noted that 10% and 1% of the diodes in the RSC are predicted to fail after 36 and 13 years of operation, respectively.

With the static equivalent values of each power device as listed in Table II, the lifetime distributions of the key IGBTs and diodes of the BTB power converters are as shown in Fig.

This article has been accepted for publication in a future issue of this journal, but has not been fully edited. Content may change prior to final publication. Citation information: DOI 10.1109/TIA.2018.2822239, IEEE Transactions on Industry Applications

7(a). It can be seen that the diode of the RSC has the lowest scale parameter of 93.3 due to its shortest static lifespan. By using the integration of the failure pdf, the accumulated failure is then shown in Fig. 7(b).

IV. System-Level Lifetime Prediction of Power Devices and Power Converters

In this section, the reliability metrics of the power converters can be assessed based on the power device level. Besides, according to thermal stresses of power devices with various paralleled power modules, the effects of power module selection on the system-level reliability design can be investigated as well.

With two low-voltage power modules in parallel of the RSC and a single power module in the GSC, although the power semiconductors in the RSC and GSC almost handle the same amount of the current at the rated power as shown in Fig. 3(b), their unreliability curves deviate significantly as seen in Fig. 7(b). In order to improve this issue, more power modules in the RSC can be paralleled, which may reduce the thermal stress of each power device and enhance its lifespan. As shown in Fig. 8, it is evident that with a higher number of paralleled power modules, the reliability of both the IGBT and diode in the RSC is considerably improved. It is worth noting that as the designed lifetime of the power semiconductor is normally less than 30 years, these unreliability curves are meaningful within the designed lifespan. Beyond the 30-year operation, the degradation related to other stressors may become dominant, which results in higher uncertainties of the lifetime prediction.

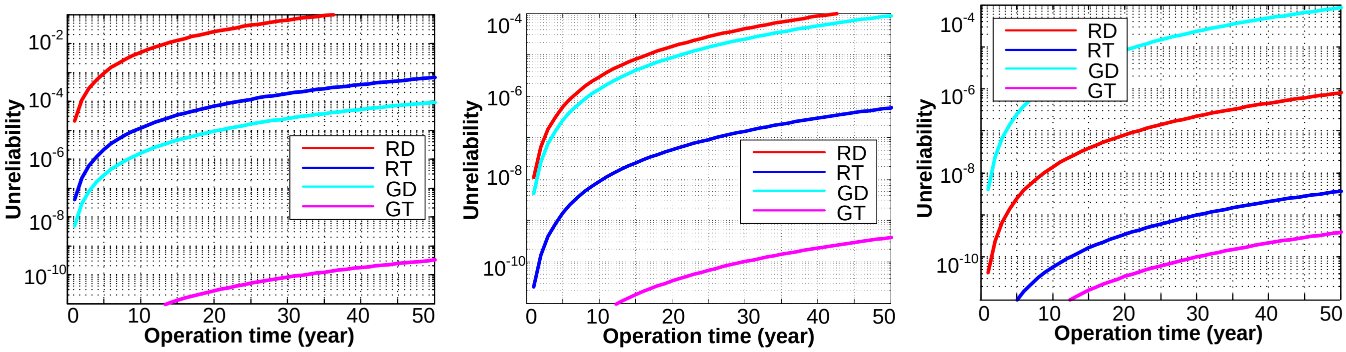

Fig. 8. Unreliability curve of diodes and IGBTs in the back-to-back power converters with various paralleled power modules in the rotor-side converter. (a) Two modules. (b) Three modules. (c) Four modules.

In order to assess the reliability metrics of the BTB power converters in the DFIG system, it starts with the reliability analysis of the GSC and RSC. The existence of any failed IGBT or diode results in abnormal operation of the power converter, which indicates that all power semiconductors are connected in series in the reliability block diagram. As the reliability of the series blocks is the product of all components, the unreliability function of the RSC F_{RSC} or GSC F_{GSC} can be expressed by the component unreliability function given as,

$$F_{RSC}(t) = 1 - \prod_{j}(1 - \mathrm{F}_{\mathrm{RD}(j)}(t))(1 - \mathrm{F}_{\mathrm{RT}(j)}(t)) \approx \sum_{j}(\mathrm{F}_{\mathrm{RD}(j)}(t) + \mathrm{F}_{\mathrm{RT}(j)}(t)) \quad (7)$$

$$F_{GSC}(t) = 1 - \prod_{k}(1 - \mathrm{F}_{\mathrm{GD}(k)}(t))(1 - \mathrm{F}_{\mathrm{GT}(k)}(t)) \approx \sum_{k}(\mathrm{F}_{\mathrm{GD}(k)}(t) + \mathrm{F}_{\mathrm{GT}(k)}(t)) \quad (8)$$

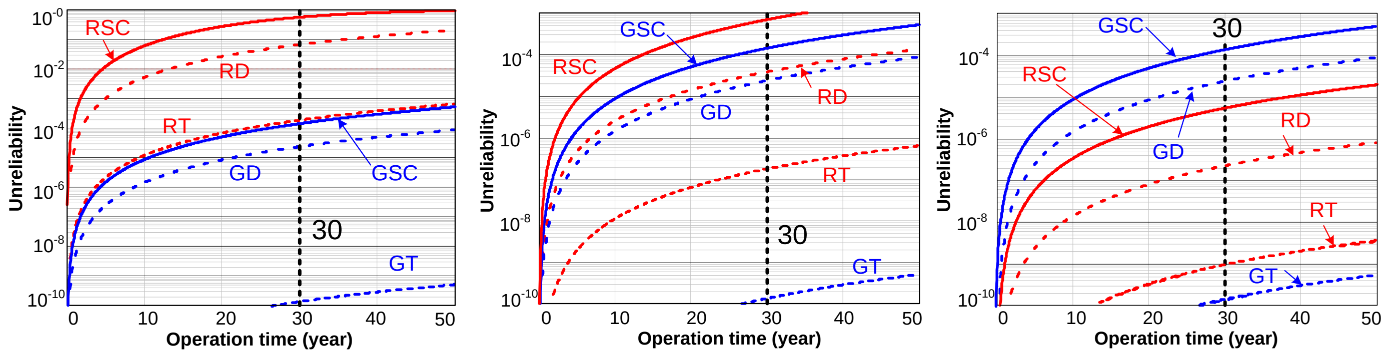

Fig. 9. Unreliability from power devices to power converter with the same design of the grid-side converter. (a) Two modules in rotor-side converter. (b) Three modules in rotor-side converter. (c) Four modules in rotor-side converter.

This article has been accepted for publication in a future issue of this journal, but has not been fully edited. Content may change prior to final publication. Citation information: DOI 10.1109/TIA.2018.2822239, IEEE Transactions on Industry Applications

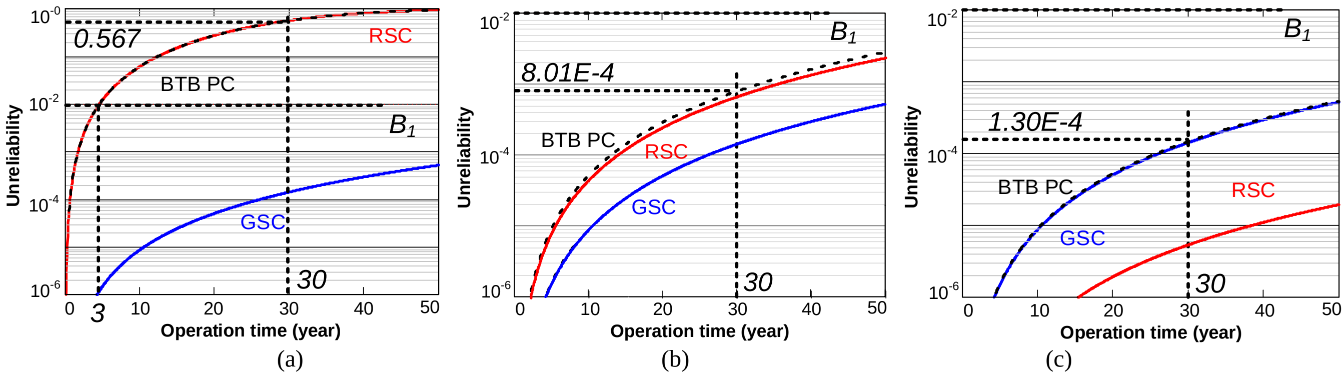

Fig. 10. Unreliability from the Rotor-Side Converter (RSC) and the Grid-Side Converter (GSC) to Back-To-Back Power Converters (BTB PC) with various power modules in the RSC. (a) Two modules. (b) Three modules. (c) Four modules.

where F_{RD} and F_{RT} denote the unreliability of the diode and the IGBT in the RSC, while F_{GD} and F_{GT} denote the unreliability of the diode and the IGBT in the GSC, j and k denote the number of the power semiconductors used in RSC and GSC. It can be seen that the increase of the paralleled power module helps to improve the reliability of the individual power semiconductor, but it may weaken the system-level reliability due to the increased number of power components.

On the basis of (7) and (8), the unreliability curves from the power device to the RSC and GSC can be calculated and it is shown in Fig. 9. It is obvious that 30-year operation of the GSC gives the damage of 1.42E-4, which is much higher than the most stressed GSC diode of 2.37E-5. In respect to the RSC, 30-year operation of the two, three and four power modules in parallel consumes the unreliability of 5.67E-1, 6.90E-4, and 5.40E-6, respectively.

Similarly, the reliability of the BTB Power Converter (BTB PC) is the series connection of the RSC and the GSC, and its unreliability curve is calculated in Fig. 10 with different solutions of paralleled power modules in the RSC. In the case of two paralleled power modules, the B_1 lifetime of the power converter system is only 3 years, which is much less than the preferred lifespan of 30 years for the modern standard of wind turbines. If three and four power modules are selected, the B_1 lifetime of the power converter is both higher than 50 years, and the designed 30-year operation contributes to 8.01E-4 and 1.30E-4 lifetime consumption. Since the reliability of other critical components (e.g. dc-link capacitors, gate drivers, etc.) is not taken into account, it is reasonable that the 30-year operation of the power semiconductors consumes less than 1% lifetime. Consequently, the selection of the three power modules is the most appropriate design seen from a reliability perspective, as the reliability curves between the RSC and the GSC is more balanced, and it closely fulfills the lifetime target. It is noted that the selection of the power modules may be different from a reliability point of view compared to the current margin of power devices, where two paralleled power modules are the best selection.

V. Conclusion

A system-level reliability analysis of back-to-back wind power converters used in the doubly-fed induction generator is described in this paper. The mission profile and Weibull distribution based approach is used to investigate the long-term electro-thermal stress profile and time-to-failure distribution of the key power semiconductors. A system-level reliability study of 2 MW wind turbine system is presented with different selections of power modules within the back-to-back power converters. Viewed from a similar margin of the current stress in the grid-side converter and the rotor-side converter, their B_1 lifetime deviates significantly. The corresponding lifetime of the back-to-back power converters lasts only 3 years, which is much lower than the industry standard of 30 years. Meanwhile, viewed from a reliability perspective, different selections of power modules can be applied. The B_1 lifetime of the grid-side converter and the rotor-side converter are increased and more balanced, which results in an improved system-level reliability.

References

[1] F. Blaabjerg, and K. Ma, "Future on power electronics for wind turbine systems," *IEEE Journal of Emerging and Selected Topics in Power Electronics*, vol. 1, no. 3, pp. 139-152, Sep. 2013.

[2] H. Polinder, J. A. Ferreira, B. B. Jensen, A. B. Abrahamsen, K. Atallah, and R. A. McMahon, "Trends in wind turbine generator systems," *IEEE Journal of Emerging and Selected Topics in Power Electronics*, vol. 1, no. 3, pp. 174-185, Sep. 2013.

[3] H. Wang, M. Liserre, F. Blaabjerg, P. Rimmen, J. Jacobsen, T. Kvisgaard, and J. Landkildehus, "Transitioning to physics-of-failure as a reliability driver in power electronics," *IEEE Journal of Emerging and Selected Topics in Power Electronics*, vol. 2, no. 1, pp. 97-114, Mar. 2014.

[4] M. Liserre, R. Cardenas, M. Molinas, and J. Rodriguez, "Overview of multi-MW wind turbines and wind parks," *IEEE Trans. on Industrial Electronics*, vol. 58, no. 4, pp. 1081-1095, Apr. 2011.

[5] "ZVEI - Handbook for robustness validation of automotive electrical/electronic modules," Jun. 2013.

[6] R. Schuerger, R. Arno, and N. Dowling, "Why existing utility metrics do not work for industrial reliability analysis," *IEEE Trans. on Industry Applications*, vol. 52, no. 4, pp. 2801-2806, Jul. 2016.

[7] P. D. T. O'Connor, and A. Kleyner, *Practical Reliability Engineering (fifth edition)*. New York, USA: Wiley, 2012.

[8] H. S. Chung, H. Wang, F. Blaabjerg, and M. Pecht, *Reliability of power electronic converter systems*. IET Publisher, 2015.

[9] S. H. Ali, M. Heydarzadeh, S. Dusmez, X. Li, A. Kamath, and B. Akin, "Lifetime estimation of discrete IGBT devices based on Gaussian process," *IEEE Trans. on Industry Applications*, IEEE early access.

[10] D. I. Stroe, M. Swierczynski, A. I. Stroe, R. Laerke, P. C. Kjaer, and R. Teodorescu, "Degradation behavior of Lithium-Ion batteries based on lifetime models and field measured frequency regulation mission profile," *IEEE Trans. on Industry Applications*, vol. 52, no. 6, pp. 5009-5018, Nov. 2016.

[11] F. J. T. E. Ferreira, G. Baoming, and A. T. de Almeida, "Reliability and operation of high-efficiency induction motors," *IEEE Trans. on Industry Applications*, vol. 52, no. 6, pp. 4628-4637, Nov. 2016.

[12] D. Zhou, F. Blaabjerg, M. Lau, and M. Tonnes, "Optimized reactive power flow of DFIG power converters for better reliability performance considering grid codes," *IEEE Trans. on Industrial Electronics*, vol. 62, no. 3, pp. 1552-1562, Mar. 2015.

[13] ABB Application Note, *Load-cycling capability of HiPak IGBT modules*, 2012.

[14] G. Zhang, D. Zhou, J. Yang, and F. Blaabjerg. "Fundamental-frequency and load-varying thermal cycles effects on lifetime estimation of DFIG power converter," *Microelectronics Reliability*, vol. 76, pp. 549-555, 2017.

[15] D. Zhou, F. Blaabjerg, M. Lau, and M. Tonnes, "Thermal behavior optimization in multi-MW wind power converter by reactive power circulation," *IEEE Trans. on Industry Applications*, vol. 50, no. 1, pp. 433-440, Jan. 2014.

[16] Military Handbook: *Reliability Prediction of Electronic Equipment, Standard MIL-HDBK-217F*, Dec. 1991.

[17] J. Harms, Revision of MIL-HDBK-217, *Reliability Prediction of Electronic Equipment*, 2010.

[18] ReliaSoft Corporation, "*Life data analysis reference*," [Online]. http://reliawiki.org/index.php/Life_Data_Analysis_Reference_Book, 2015.

[19] A. Khosroshahi, M. Abapour, and M. Sabahi, "Reliability evaluation of conventional and interleaved DC–DC boost converters," *IEEE Trans. on Power Electronics*, vol. 30, no. 10, pp. 5821-5828, Oct. 2015.

[20] A. M. Bazzi, A. Dominguez-Garcia, and P. T. Krein, "Markov reliability modeling for induction motor drives under field-oriented control," *IEEE Trans. on Power Electronics*, vol. 27, no. 2, pp. 534-546, Feb. 2012.

[21] M. Tanrioven, and M. S. Alam, "Reliability modeling and analysis of stand-alone PEM fuel cell power plants." *Renewable Energy*, vol. 31, no. 7, pp. 915-933, 2006.

[22] X. Yu, and A. M. Khambadkone, "Reliability analysis and cost optimization of parallel-inverter system," *IEEE Trans. on Industrial Electronics*, vol. 59, no. 10, pp. 3881-3889, Oct. 2012.

[23] L. Placca, and R. Kouta. "Fault tree analysis for PEM fuel cell degradation process modelling." *International Journal of Hydrogen Energy*, vol. 36, no. 19, pp. 12393-12405, 2011.

[24] D. Zhou, H. Wang, and F. Blaabjerg, "Mission profile based system-level reliability analysis of DC/DC converters for a backup power application," *IEEE Trans. on Power Electronics*, IEEE early access.

[25] D. Zhou, G. Zhang, and F. Blaabjerg, "Design of power converter in DFIG wind turbine with enhanced system-level reliability," *in Proc. of IEEE ECCE 2017*, pp.1-8, 2016.

[26] R. Bayerer, T. Hermann, T. Licht, J. Lutz, and M. Feller, "Model for power cycling lifetime of IGBT modules—various factors influencing lifetime," *in Proc. of Integrated Power Systems (CIPS) 2008*, pp.1-6, 2008.

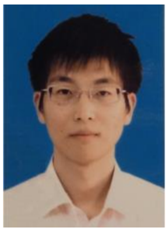

Dao Zhou (S'12, M'15) received the B.S. from Beijing Jiaotong University, Beijing, China, in 2007, the M. S. from Zhejiang University, Hangzhou, China, in 2010, and the Ph.D. from Aalborg University, Aalborg, Denmark, in 2014, all in electrical engineering.

Since 2014, he has been with Department of Energy Technology, Aalborg University, where currently he is an Assistant Professor. His research interests include modeling, control, and reliability of power electronics in renewable energy application.

Guanguan Zhang (S'15) received the B.S. degree from Central South University, Changsha, China, in 2012, where she is working toward the Ph.D. degree in power electronics and power transmission. She was a joint Ph.D. student supported by the China Scholarship Council with the Department of Energy Technology, Aalborg University, Aalborg, Denmark, where she focuses on the reliability analysis of wind power system.

Her research interests include matrix converter, motor control and wind power system.

Frede Blaabjerg (S'86-M'88-SM'97-F'03) was with ABB-Scandia, Randers, Denmark, from 1987 to 1988. From 1988 to 1992, he got the Ph.D. degree in Electrical Engineering at Aalborg University in 1995. He became an Assistant Professor in 1992, an Associate Professor in 1996, and a Full Professor of power electronics and drives in 1998. From 2017 he became a Villum Investigator.

His current research interests include power electronics and its applications such as in wind turbines, PV systems, reliability, harmonics and adjustable speed drives. He has published more than 500 journal papers in the fields of power electronics and its applications. He is the co-author of two monographs and editor of 6 books in power electronics and its applications.

He has received 24 IEEE Prize Paper Awards, the IEEE PELS

This article has been accepted for publication in a future issue of this journal, but has not been fully edited. Content may change prior to final publication. Citation information: DOI 10.1109/TIA.2018.2822239, IEEE Transactions on Industry Applications

Distinguished Service Award in 2009, the EPE-PEMC Council Award in 2010, the IEEE William E. Newell Power Electronics Award 2014 and the Villum Kann Rasmussen Research Award 2014. He was the Editor-in-Chief of the IEEE TRANSACTIONS ON POWER ELECTRONICS from 2006 to 2012. He has been Distinguished Lecturer for the IEEE Power Electronics Society from 2005 to 2007 and for the IEEE Industry Applications Society from 2010 to 2011 as well as 2017 to 2018. He is nominated in 2014, 2015, 2016 and 2017 by Thomson Reuters to be between the most 250 cited researchers in Engineering in the world. In 2017 he became Honoris Causa at University Politehnica Timisoara (UPT), Romania.